



## Decolorization of an azo dye Orange G in microbial fuel cells using Fe(II)-EDTA catalyzed persulfate

Cheng-Gang Niu <sup>\*</sup>, Ying Wang, Xue-Gang Zhang, Guang-Ming Zeng, Da-Wei Huang, Min Ruan, Xiang-Wei Li

College of Environmental Science and Engineering, Hunan University, Changsha 410082, PR China

Key Laboratory of Environmental Biology and Pollution Controls Hunan University, Ministry of Education, Changsha 410082, PR China

### HIGHLIGHTS

- ▶ Microbial fuel cell using Fe(II)-EDTA catalyzed persulfate as the cathode solution.
- ▶ Microbial fuel cell degraded OG and harvest electricity simultaneously.
- ▶ The decolorization kinetics of OG followed the second-order kinetics well.
- ▶ EDTA could improve the stability of voltage output.

### ARTICLE INFO

#### Article history:

Received 7 May 2012

Received in revised form 30 August 2012

Accepted 1 September 2012

Available online 8 September 2012

#### Keywords:

Microbial fuel cell

Fe(II)-EDTA catalyzed persulfate

Orange G decolorization

Maximum power density

### ABSTRACT

This study constructed a microbial fuel cell (MFC) using Fe(II)-EDTA catalyzed persulfate as the cathode solutions to decolorize Orange G (OG) and harvest electricity simultaneously. Chelated Fe<sup>2+</sup> could activate persulfate to generate sulfate free radicals (SO<sub>4</sub><sup>-</sup>) which with high oxidation potential ( $E^0 = 2.6$  V) can degrade azo dyes. The influence of some important factors such as pH value of cathode solutions, dosages of K<sub>2</sub>S<sub>2</sub>O<sub>8</sub>, Fe<sup>2+</sup> and EDTA were investigated in a two-chamber microbial fuel cell. Under an optimal condition, the maximum power density achieved 91.1 mW m<sup>-2</sup>, the OG removal rate was 97.4% and the K<sub>2</sub>S<sub>2</sub>O<sub>8</sub> remaining rate was 47.3% after 12 h. The OG degradation by Fe(II)-EDTA catalyzed persulfate was found to follow the second-order kinetic model.

© 2012 Elsevier Ltd. All rights reserved.

### 1. Introduction

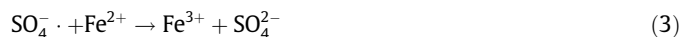
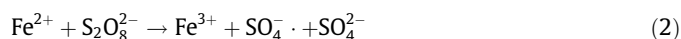
Azo dyes are characterized by the presence of one or more azo bonds (–N=N–) in association with aromatic systems and auxochromes (–OH, –SO<sub>3</sub>, etc.). Azo dyes represent more than 50% of all dyes in common use because of their chemical stability and versatility, and most of them are non-biodegradable, toxic and potentially carcinogenic in nature (Figueroa et al., 2009; Bakhshian et al., 2011). The widespread utilization of azo dyes has caused an important environmental problem (Gupta and Suhas, 2009). Many wastewater treatment technologies have been applied for the removal of azo dyes from aqueous solutions including physical, chemical, and biological processes (Yuan et al., 2011; Wu and Wang, 2001; Sun et al., 2006). Nevertheless, these methods are

inefficient and costly for removing dyes from wastewater (Sun et al., 2009). In recent years, advanced oxidation processes (AOPs) have been widely developed as promising and efficient methods to treat these dyes such as Fenton reaction (Fu et al., 2010), TiO<sub>2</sub>-mediated photocatalysis (Yu et al., 2008) and other oxidative reactions using persulfate with ferrous ion (Xu and Li, 2010). AOPs are based on *in situ* generation of very powerful oxidizing agent such as hydroxyl radical, which has one unpaired electron and was highly effective for removing organic dyes from water.

Fe<sup>2+</sup> activated persulfate degradation of OG (a typical azo dye in textile wastewaters) has been reported (Xu and Li, 2010), and the reactions in accordance with Eqs. (1)–(3) (Kolthoff et al., 1951):



Through the steps:



<sup>\*</sup> Corresponding author at: College of Environmental Science and Engineering, Hunan University, Changsha, Hunan 410082, PR China. Tel.: +86 731 88823820.

E-mail addresses: [cgniu@hotmail.com](mailto:cgniu@hotmail.com), [cgniu@hnu.edu.cn](mailto:cgniu@hnu.edu.cn) (C.-G. Niu).

**Table 1**  
Physiochemical characteristics of Orange G.

Dye	Chemical structure	Molecular formula	MW(g mol <sup>-1</sup> )	$\lambda_{\max}$ (nm)
Orange G		C <sub>16</sub> H <sub>10</sub> N <sub>2</sub> Na <sub>2</sub> O <sub>7</sub> S <sub>2</sub>	452	478

Ferrous ion can activate persulfate anion to produce the sulfate free radical (SO<sub>4</sub><sup>-</sup>) with a standard redox potential ( $E^0$ ) of 2.6 V. The sulfate free radicals with high oxidation potential can degrade organic contaminants such as lindane and trichloroethylene (Liang et al., 2004a; Cao et al., 2008). However, extensive persulfate consumption resulted from the presence of excess Fe<sup>2+</sup>, which was not necessarily for contaminants degradation (Liang et al., 2004a). It was postulated that chelating agents can regulate and maintain Fe<sup>2+</sup> activity as an activator for persulfate (Liang et al., 2004b). EDTA is most importantly used in industrial processes among a variety of chelating agents (Pirkanniemi et al., 2007). Minimization of free Fe<sup>2+</sup> by EDTA, and the resulting slow generation of SO<sub>4</sub><sup>-</sup>, can be beneficial in reducing peroxide consumption and can increase contaminant degradation efficiency.

Microbial fuel cell (MFC) was explored to treat azo dye containing wastewater (Hou et al., 2011; Liu et al., 2009), which is an emerging technology for wastewater treatment and energy production simultaneously (Cusick et al., 2010; Wang et al., 2011). The most remarkable advantage of MFC is its ability to generate combustion-less, pollution-free bioelectricity directly from biodegradable compounds by utilizing bacteria as catalysts (Rittmann, 2008). This study constructed a double-chamber MFC to improve the decolorization efficiency of OG and harvest electricity at the same time. Fe(II)-EDTA activated persulfate was used to reduce OG in cathode chamber. The authors investigated the influences of some important factors such as pH value of cathode solutions, dosages of K<sub>2</sub>S<sub>2</sub>O<sub>8</sub>, Fe<sup>2+</sup> and EDTA on the OG degradation and power generation in aqueous solution. Furthermore, the kinetics of OG degradation by Fe(II)-EDTA activated persulfate was elucidated based on the experimental data.

## 2. Methods

### 2.1. Chemicals

The Orange G was purchased from Sangon Biotechnology Co., Ltd. (Shanghai, China) and its physiochemical characteristics are shown in Table 1. The excess activated sludge used in the anode chamber was obtained from the Second Wastewater Treatment of Changsha City in China. All other chemicals were analytic grade and purchased from Sinopharm Chemical Reagent Co., Ltd. (Shanghai, China)

### 2.2. MFC configuration and operation

A two-chamber microbial fuel cell used in the present study was made of plexiglas and built in a traditional "H" shape. The MFC consist of an anaerobic anode chamber and an aerobic cathode chamber which are usually separated by proton exchange membrane (PEM, Nafion™ 117, Dupont Co., USA). The anode chamber was anaerobic while the cathode chamber was open to the air; each chamber has an effective volume of 250 mL. Substrate is oxidized by bacteria generating electrons and protons at the anode

chamber. The protons travelling through the PEM and the electrons travelling through the external circuit are combined with electron acceptors at the cathode chamber. The flow of electron and proton in MFC was shown in Fig. S1. Prior to use, the PEM was pretreated by boiling in H<sub>2</sub>O<sub>2</sub> (30%) and deionized water, followed by 0.5 mol L<sup>-1</sup> H<sub>2</sub>SO<sub>4</sub> and deionized water, each for 1 h, and then was stored in deionized water. Graphite rods with a projected surface area of 13.1 cm<sup>2</sup> (of 50.0 mm in length and 8.0 mm diameter) were used as the anode electrode and the cathode electrode.

All MFCs were conducted in batch-fed mode at a load of 1,000 Ω (unless stated otherwise) at the temperature of 30 °C. MFCs were inoculated with 100 mL excess activated sludge and 150 mL artificial wastewater (glucose 1 g L<sup>-1</sup>, NaH<sub>2</sub>PO<sub>4</sub>·2H<sub>2</sub>O 5.618 g L<sup>-1</sup>, Na<sub>2</sub>HPO<sub>4</sub>·12H<sub>2</sub>O 6.150 g L<sup>-1</sup>, NH<sub>4</sub>Cl 0.31 g L<sup>-1</sup>, KCl 0.13 g L<sup>-1</sup>, trace mineral 12.5 mL L<sup>-1</sup> and vitamin solutions 12.5 mL L<sup>-1</sup> (Lovely and Phillips, 1988), pH 7.0). After replacement of this feed solution twice over three days, the reactors were then operated using only artificial wastewater in the anode chamber. When the maximum voltage was reproducible at least three times, the MFC was considered fully acclimated. During the experiment, the anode chamber was filled with 250 mL artificial wastewater. The cathode solution consisted of EDTA, FeSO<sub>4</sub>·7H<sub>2</sub>O, persulfate and OG, the initial concentration of OG was maintained 0.1 mmol L<sup>-1</sup> during the operation. A predetermined amount of OG solution was prepared for the cathode solution, premixed EDTA and Fe<sup>2+</sup> solution was added to the contaminant solution (OG). The resulting solution was mixed for a few minutes, and then K<sub>2</sub>S<sub>2</sub>O<sub>8</sub> was added and mixed briefly. Additionally, the experiment with only Fe<sup>2+</sup> and dye in the cathode solutions was investigated, the degradation of Orange G could not be found under this condition.

### 2.3. Analytical methods

Voltage ( $E$ ) was measured at 30 min intervals by a multimeter (UNI-T 803; Uni-Trend Electronics Co., Ltd., Shanghai, China) connected to a personal computer. Current density ( $I_A$ ) and power density ( $P$ ) were obtained according to  $I_A = E/RA$  and  $P = EI/A$ , where  $E$  is the voltage,  $R$  is the electrical resistance,  $I$  is the current, and  $A$  is the surface area of the electrode. In order to obtain the power density curves, external circuit resistances were varied from 9000 Ω to 100 Ω in a decreasing order. Potassium persulfate concentration (Frigerio, 1963) and OG concentration were analyzed by a Shimadzu UV-2550 spectrophotometer. The pH values were measured with a pH meter (pHS-25; Shanghai Rex Xinjing Instrument Co., Ltd., Shanghai, China).

## 3. Results and discussion

### 3.1. OG degradation

Fe(II)-EDTA activated persulfate for OG degradation was investigated in this experiment. The spectrum of light absorption by the OG solution showed three main peaks at 248 nm, 330 nm, and

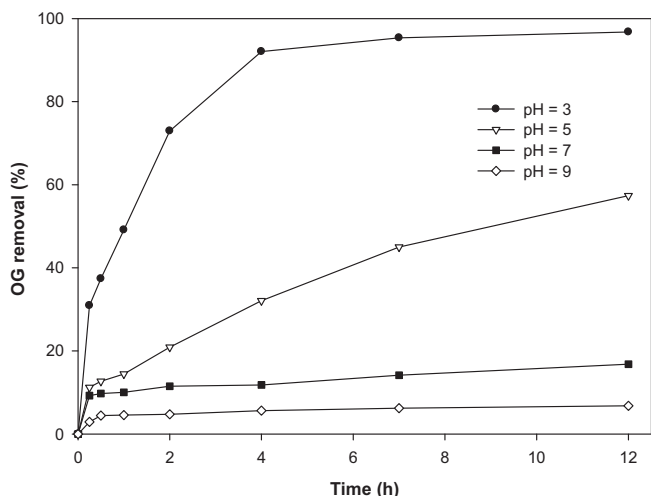


**Fig. 1.** Degradation rates of OG at different MFCs with  $S_2O_8^{2-}/Fe^{2+}/EDTA/OG$  at the molar ratios of 2:1:1:0.1,  $[OG] = 0.1 \text{ mmol L}^{-1}$ .

478 nm. The peak at 478 nm was attributed to the absorption of the  $n \rightarrow \pi^*$  transition related to the  $-N=N-$  group in OG molecule, while the peaks at 248 nm and 330 nm were assigned to its aromatic rings (Sun et al., 2009; Deng et al., 2009). The extent of OG decolorization was evaluated by measuring the absorption intensity of solution at 478 nm. UV-Vis absorption spectra of the reaction solution with Fe(II)-EDTA activated persulfate revealed that with the color removed from the cathode solution, the absorbance in the visible region at 478 nm for OG was decreased during 12 h of operation (Fig. S2). This indicated that azo bonds ( $-N=N-$ ) were destroyed by Fe(II)-EDTA catalyzed persulfate.

### 3.2. Optimization of system influencing factors for OG decolorization and power generation in MFC

#### 3.2.1. Effect of pH for OG decolorization

The pH value of aqueous solution plays a significant role in organic compounds degradation. This paper investigated the effect of initial pH value of cathode solutions on OG degradation in the MFCs with  $S_2O_8^{2-}/Fe^{2+}/EDTA/OG$  at the initial molar ratios of 2:1:1:0.1 ( $[OG] = 0.1 \text{ mmol L}^{-1}$ ). The cathode solutions of different MFCs were carried out at initial pH from 3.0 to 9.0. As shown in Fig. 1, the efficiency of OG degradation decreased with the increase of pH. The maximum OG degradation rate of 96.8% was achieved in the MFC with the initial pH value of 3.0. The OG degradation rates of MFCs with different initial pH at 5.0, 7.0 and 9.0 were 57.4%, 16.8% and 6.8%, respectively. Acidic pH condition was more favorable to the OG degradation than neutral pH and alkaline pH. This might result from the formation of ferrous/ferric hydroxide complexes ( $pH > 4$ ) which are poor activators for persulfate led to decrease of the  $SO_4^-$  amount (Liang et al., 2009). It is obviously that OG could not be removed effectively at the pH from 5.0 to 9.0. Therefore the best initial pH for the following experiments of OG degradation in this study was 3.0.

#### 3.2.2. Effect of potassium persulfate dosage on OG decolorization and power generation

Persulfate as a source of  $SO_4^-$  generation plays an important role in the cathode reaction. The experiment was carried out at constant initial dosages of  $Fe^{2+}$ , EDTA and OG, but 4 levels of  $K_2S_2O_8$  concentrations in cathode chambers. The effect of  $K_2S_2O_8$  dosage on the decolorization of OG was examined by varying initial concentration of  $K_2S_2O_8$  from 0.0 to  $8.0 \text{ mmol L}^{-1}$  and the results were shown in Fig 2A. Compared to the MFC without persulfate, the removal rates of OG in MFCs using persulfate are much better. The OG removal rate in MFC without  $K_2S_2O_8$  was 13%. It can be

observed that with the persulfate dosage increasing resulted only a slight improving in the OG removal. The OG removal rates were 96.8%, 97.4% and 98.2% after 12 h respectively when the initial concentration of  $K_2S_2O_8$  were 2.0, 4.0 and  $8.0$ .

In addition to influence the efficiency of OG degradation, the  $K_2S_2O_8$  dosage also affected the power generation significantly. From Fig. 2B, we can see that the maximum power density of MFC was improving with the increasing of initial  $K_2S_2O_8$  concentration. The maximum power density of MFCs were of  $21.8 \text{ mW m}^{-2}$ ,  $35.1 \text{ mW m}^{-2}$ ,  $91.1 \text{ mW m}^{-2}$  and  $191.6 \text{ mW m}^{-2}$  in the presence of  $0.0 \text{ mmol L}^{-1}$ ,  $2.0 \text{ mmol L}^{-1}$ ,  $4.0 \text{ mmol L}^{-1}$  and  $8.0 \text{ mmol L}^{-1}$  of  $K_2S_2O_8$ . The results indicated that persulfate was propitious for both OG degradation and power putout. However, in order to obtain better performance with less  $K_2S_2O_8$  dosage,  $4.0 \text{ mmol L}^{-1}$   $K_2S_2O_8$  was selected for the following experiments.

#### 3.2.3. Effect of ferrous ion dosage on OG decolorization and power generation

$Fe^{2+}$  is another important factor in cathode reaction which catalytically decomposes  $K_2S_2O_8$  to  $SO_4^-$ . The experiment was carried out at constant initial dosages of  $K_2S_2O_8$ , EDTA and OG, but 4 levels of  $Fe^{2+}$  concentrations in cathode chambers, the varying initial  $Fe^{2+}$  concentration were of  $0.0 \text{ mmol L}^{-1}$ ,  $0.5 \text{ mmol L}^{-1}$ ,  $1 \text{ mmol L}^{-1}$  and  $2.0 \text{ mmol L}^{-1}$ . Fig. 3A showed the effect of  $Fe^{2+}$  dosage on the decolorization of OG. A great improvement of the decolorization of OG could be observed in the presence of  $Fe^{2+}$  with  $0.0 \text{ mmol L}^{-1}$ ,  $0.5 \text{ mmol L}^{-1}$ ,  $1.0 \text{ mmol L}^{-1}$  and  $2.0 \text{ mmol L}^{-1}$ , the decolorization

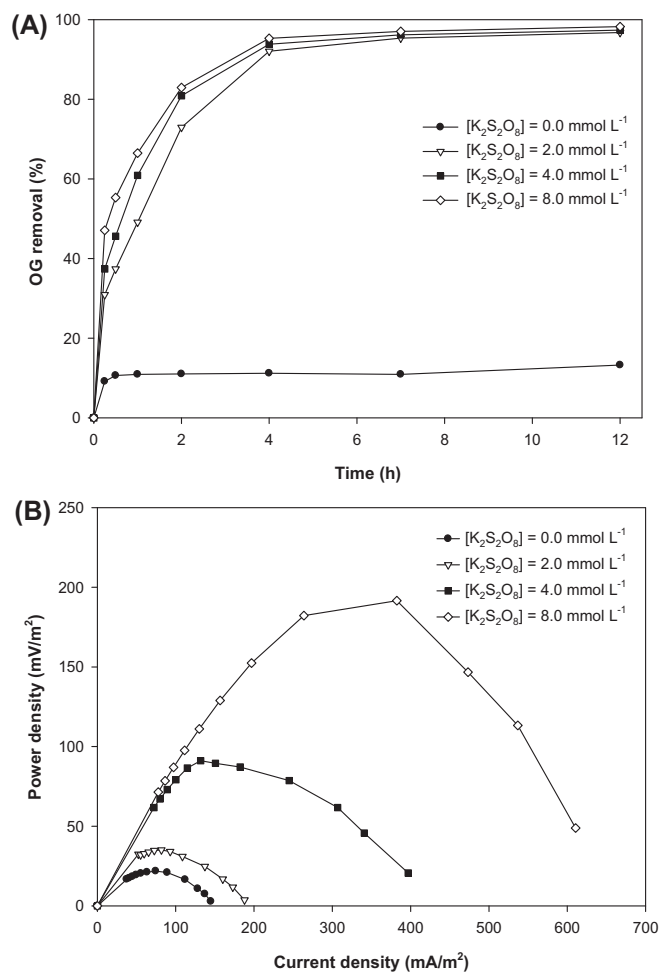


**Fig. 2.** OG degradation rates (A) and power density curves (B) with different initial persulfate concentration in cathode chambers.  $[OG] = 0.1 \text{ mmol L}^{-1}$ ,  $[Fe^{2+}] = 1.0 \text{ mmol L}^{-1}$ ,  $[EDTA] = 1.0 \text{ mmol L}^{-1}$ .

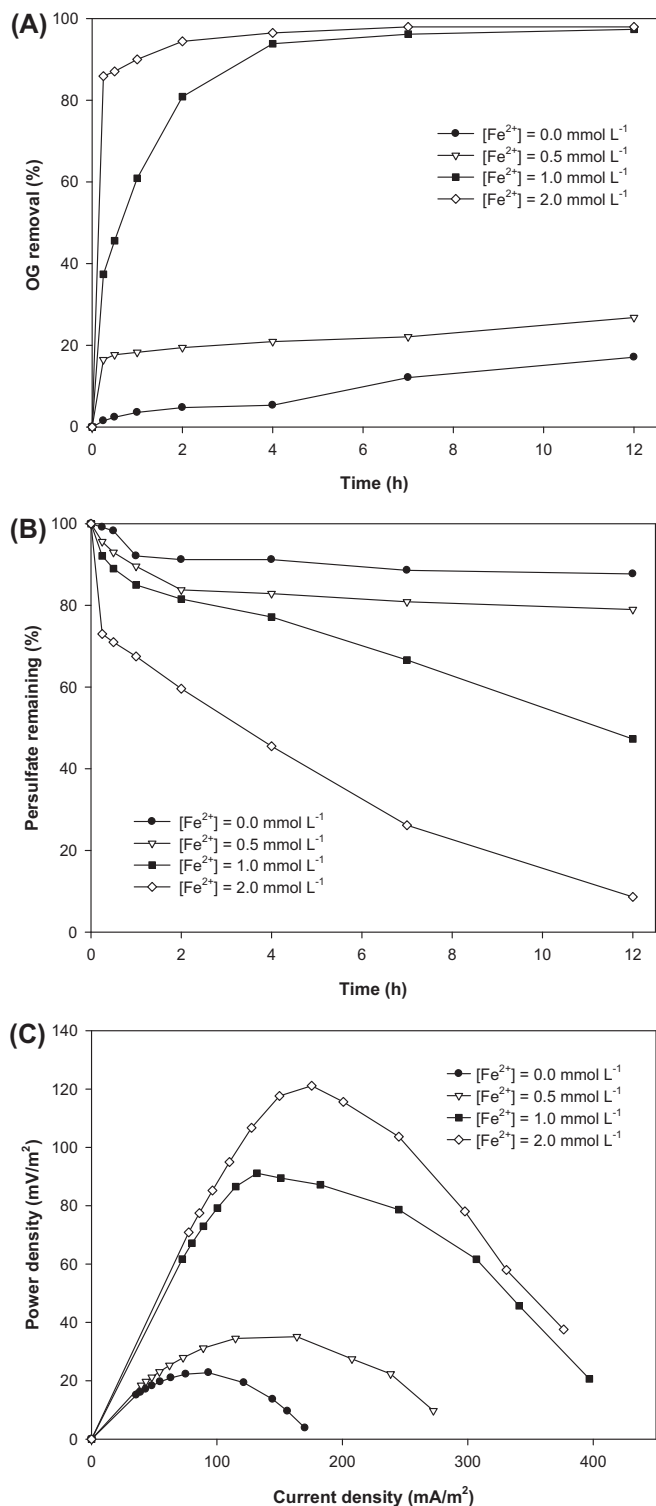


**Fig. 3.** OG degradation rates (A), persulfate remaining rates (B) and power density curves (C) with different initial  $\text{Fe}^{2+}$  concentration in cathode chambers.  $[\text{OG}] = 0.1 \text{ mmol L}^{-1}$ ,  $[\text{K}_2\text{S}_2\text{O}_8] = 4.0 \text{ mmol L}^{-1}$ ,  $[\text{EDTA}] = 1.0 \text{ mmol L}^{-1}$ .

efficiencies within 12 h of reaction were 17.1%, 26.8%, 97.4% and 97.9%, respectively. Higher decolorization efficiencies achieved with more initial  $\text{Fe}^{2+}$  concentration, which was chiefly attribute to more generation of  $\text{SO}_4^-$  with more  $\text{Fe}^{2+}$  in cathode reaction. It is obviously that OG can be removed effectively when the initial dosage of  $\text{Fe}^{2+}$  more than  $1.0 \text{ mmol L}^{-1}$ . This study also investigated the persulfate remaining rates with different initial  $\text{Fe}^{2+}$

concentrations (Fig 3B). It can be seen that more  $\text{Fe}^{2+}$  consumed more persulfate.

The power generation of MFCs with different initial  $\text{Fe}^{2+}$  concentration was illustrated in Fig 3C. The maximum power density was highest for the MFC using  $2.0 \text{ mmol L}^{-1} \text{ Fe}^{2+}$  ( $121.1 \text{ mW m}^{-2}$ ), followed by  $1.0 \text{ mmol L}^{-1} \text{ Fe}^{2+}$  ( $91.1 \text{ mW m}^{-2}$ ),  $0.5 \text{ mmol L}^{-1} \text{ Fe}^{2+}$  ( $35.1 \text{ mW m}^{-2}$ ) and absence of  $\text{Fe}^{2+}$  ( $22.8 \text{ mW m}^{-2}$ ). These results indicated that variations in power generation during azo dye decolorization are associated with  $\text{Fe}^{2+}$  dosage used in MFCs. Ferrous ion can activate persulfate anion to produce the sulfate free radical. According to Eqs. (4) and (5), sulfate free radical with a standard redox potential of 2.6 V which is higher than that of  $\text{S}_2\text{O}_8^{2-}$  (2.01 V).



The increasing concentration of  $\text{Fe}^{2+}$  contributed to the generation of sulfate free radicals that would increase power output in MFC, whereas consumed more  $\text{K}_2\text{S}_2\text{O}_8$ . Herein,  $1.0 \text{ mmol L}^{-1}$  of  $\text{Fe}^{2+}$  was considered to be a suitable dosage for effective OG decolorization, higher power generation and less persulfate consumption.

### 3.2.4. Effect of EDTA dosage on OG decolorization and power generation

Chelated ferrous ion has been used as an activator for persulfate in previous studies (Liang et al., 2004b; Nadim et al., 2006), however, little is known on Fe(II)-EDTA catalyzed  $\text{K}_2\text{S}_2\text{O}_8$  to decolorize OG in MFC. Chelating agents could regulate and maintain the concentration of  $\text{Fe}^{2+}$  for persulfate oxidation of organic contaminant. The effect of initial EDTA concentration on OG degradation, persulfate consumption and power output were investigated. The experiment was carried out at constant initial dosages of  $\text{K}_2\text{S}_2\text{O}_8$ ,  $\text{Fe}^{2+}$ , OG and with 4 levels of EDTA concentrations in cathode chambers, the varying initial EDTA concentrations were  $0.0 \text{ mmol L}^{-1}$ ,  $0.5 \text{ mmol L}^{-1}$ ,  $1.0 \text{ mmol L}^{-1}$  and  $2.0 \text{ mmol L}^{-1}$ . Fig. 4A and B showed that the Fe(II)-EDTA catalyzed persulfate can effectively degrade OG and increasing EDTA concentration can reduce the consumption of persulfate. The persulfate remaining rates within 12 h of reaction were 18.2%, 17.4%, 47.3% and 82.4% when the initial concentrations of  $\text{Fe}^{2+}$  were  $0.0 \text{ mmol L}^{-1}$ ,  $0.5 \text{ mmol L}^{-1}$ ,  $1.0 \text{ mmol L}^{-1}$  and  $2.0 \text{ mmol L}^{-1}$ , respectively. However, excessive EDTA was not conducive to OG degradation in short time. EDTA minimized the free ferrous iron concentration that resulted slow generation of sulfate radical which was similar to the Fenton reactions (Li et al., 2007). This can be beneficial to reducing peroxide consumption and can increase contaminant degradation efficiency. It should be noted that small amounts of yellow precipitate has been found in cathode chamber of MFC in the absence of EDTA. This was due to the reaction between sulfate radicals and excess  $\text{Fe}^{2+}$ ,  $\text{Fe}^{2+}$  converted to  $\text{Fe}^{3+}$  by  $\text{SO}_4^-$  (Eq. (3)). Additionally, yellow precipitate could not be discovered in the MFC using EDTA. One limitation to the use of ferrous iron as an activator of persulfate is that the sulfate radicals and excess ferrous iron react so rapidly, that the sulfate radicals could be destroyed, which would obstruct the destruction of the organic contamination. The reaction showed in equation 3 was minimized by EDTA which can slowly provide small quantities of  $\text{Fe}^{2+}$ .

The slow generation of sulfate radical affected the power generation. As presented in Fig. 5A and B, increased initial EDTA concentration could decrease the maximum power density of MFC, whereas improved the stability of voltage output during the MFC operation. Based on what has been mentioned above,  $1.0 \text{ mmol L}^{-1}$

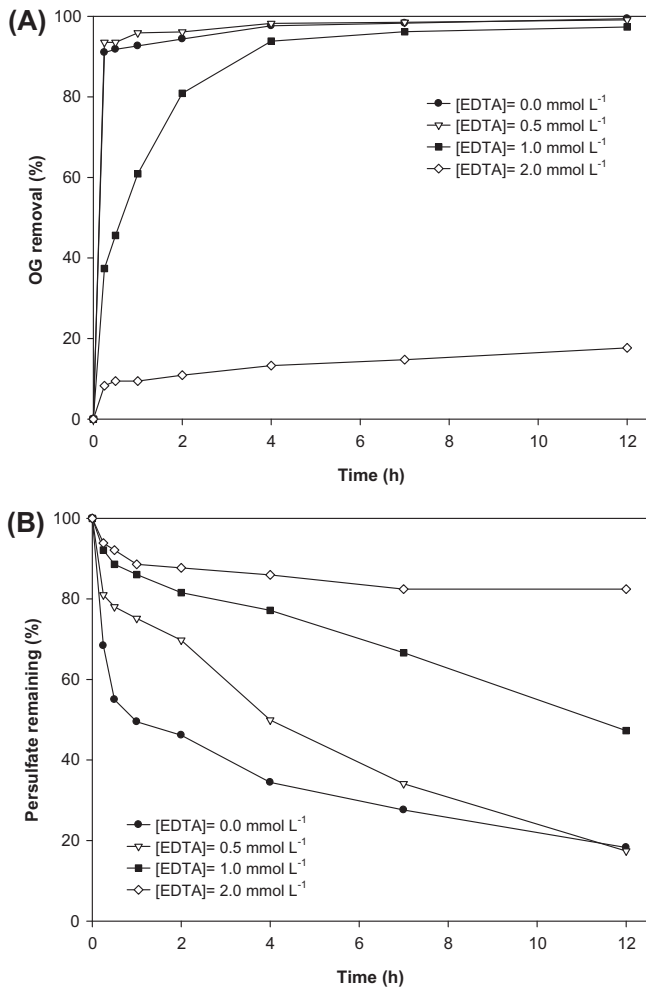


**Fig. 4.** OG degradation rates (A) and persulfate remaining rates (B) with different initial EDTA concentration in cathode chambers. [OG] = 0.1 mmol L<sup>-1</sup>, [K<sub>2</sub>S<sub>2</sub>O<sub>8</sub>] = 4.0 mmol L<sup>-1</sup>, [Fe<sup>2+</sup>] = 1.0 mmol L<sup>-1</sup>.

EDTA was selected for effective OG decolorization and stability power generation.

### 3.3. Kinetic study

Zero-, first- and second-order reaction kinetics were used to study the decolorization kinetics of OG. The individual kinetic model was presented as below:

$$C_t = C_0 - k_0 t \quad (6)$$

$$C_t = C_0 e^{-k_1 t} \quad (7)$$

$$\frac{1}{C_t} = \frac{1}{C_0} + k_2 t \quad (8)$$

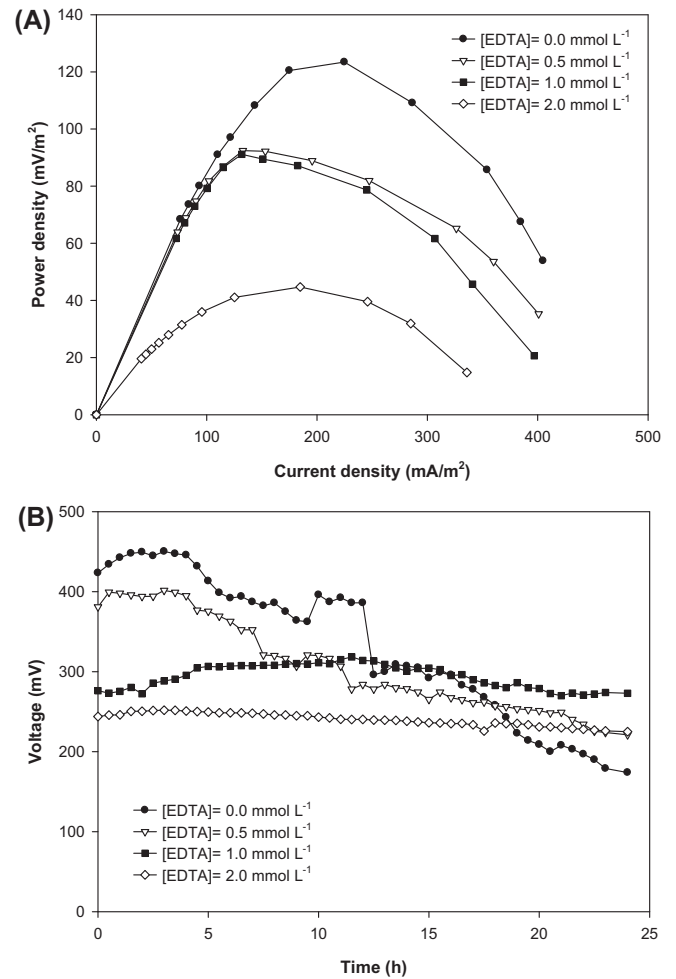


**Fig. 5.** Power density curves and voltage output of MFCs with different initial Fe<sup>2+</sup> concentrations. [OG] = 0.1 mmol L<sup>-1</sup>, [K<sub>2</sub>S<sub>2</sub>O<sub>8</sub>] = 4.0 mmol L<sup>-1</sup>, [Fe<sup>2+</sup>] = 1.0 mmol L<sup>-1</sup>.

where  $C_t$  is the concentration of OG at time  $t$ ;  $C_0$  is the initial concentration of OG;  $k_0$ ,  $k_1$  and  $k_2$  represent the apparent kinetic rate constants of zero-, first- and second-order reaction kinetics, respectively.

Comparing the regression coefficients ( $R^2$ ) obtained from Fig. S3 (A–C), it can be seen that the plot of  $1/C_t$  versus time shows a linear relationship and  $R^2$  based on the second-order reaction kinetics was 0.9827, which was obviously much better than that based on the zero-order ( $R^2 = 0.8369$ ) and the first-order ( $R^2 = 0.5446$ ) reaction kinetics. The results indicated that the decolorization kinetics of OG followed the second-order kinetics well. The apparent kinetic rate constants ( $k_2$ ) of the decolorization of OG was found to be 543.1 M<sup>-1</sup> min<sup>-1</sup> at an optimal condition of [OG] = 0.1 mmol L<sup>-1</sup>, [K<sub>2</sub>S<sub>2</sub>O<sub>8</sub>] = 4.0 mmol L<sup>-1</sup>, [Fe<sup>2+</sup>] = 1.0 mmol L<sup>-1</sup>, [EDTA] = 1.0 mmol L<sup>-1</sup>, pH = 3.0 and 30 °C. Based on the above analysis, the second-order kinetic rate constants and regression

**Table 2**

The second-order kinetic rate constants and regression coefficients for the decolorization of OG at different reaction conditions.

No.	[OG] (mM)	pH	[K <sub>2</sub> S <sub>2</sub> O <sub>8</sub> ] (mM)	[Fe <sup>2+</sup> ] (mM)	[EDTA] (mM)	Temperature (°C)	$k_2$ (M <sup>-1</sup> min <sup>-1</sup> )	$R^2$
1	0.1	3.0	2.0	1.0	1.0	30	444.05	0.9818
2	0.1	3.0	4.0	1.0	1.0	30	543.10	0.9827
3	0.1	3.0	8.0	1.0	1.0	30	798.98	0.9920
4	0.1	3.0	4.0	2.0	1.0	30	666.67	0.9206
5	0.1	3.0	4.0	1.0	0.5	30	1442.40	0.9719

coefficients for the decolorization of OG at different reaction conditions were obtained and the results were shown in Table 2. In the present study, it can be concluded that the decolorization of OG by Fe(II)-EDTA catalyzed persulfate fits the second-order reaction kinetic.

#### 4. Conclusions

Our study showed that microbial fuel cell using Fe(II)-EDTA catalyzed persulfate as the cathode solution could degrade OG efficiently and harvest electricity. EDTA could improve the stability of voltage output. Under the optimal conditions, the OG remove rates was 97.4%,  $K_2S_2O_8$  remaining rates was 47.3% and the maximum power density of MFC was  $91.1 \text{ mW m}^{-2}$  (optimal conditions:  $[OG] = 0.1 \text{ mmol L}^{-1}$ ,  $[K_2S_2O_8] = 4.0 \text{ mmol L}^{-1}$ ,  $[Fe^{2+}] = 1.0 \text{ mmol L}^{-1}$ ,  $[EDTA] = 1.0 \text{ mmol L}^{-1}$ ,  $\text{pH} = 3.0$ ). The kinetics study indicated that the decolorization kinetics of OG followed the second-order kinetics well.

#### Acknowledgements

This work was financially supported by the National Natural Science Foundation of China (20977026), the National 863 High Technology Research Foundation of China (2006AA06Z407), the Research Fund for the Doctoral Program of Higher Education of China (20090161110009), the Project-sponsored by SRF for ROCS, SEM (521294018), and the Fundamental Research Funds for the Central Universities of Hunan University (531107040375).

#### Appendix A. Supplementary data

Supplementary data associated with this article can be found, in the online version, at <http://dx.doi.org/10.1016/j.biortech.2012.09.001>.

#### References

- Bakhshian, S., Karimini, H.R., Roshandel, R., 2011. Bioelectricity generation enhancement in a dual chamber microbial fuel cell under cathodic enzyme catalyzed dye decolorization. *Bioresour. Technol.* 102, 6761–6765.
- Cao, J.S., Zhang, W.X., Brown, D.G., Sethi, D., 2008. Oxidation of lindane with Fe(II) activated sodium persulfate. *Environ. Eng. Sci.* 25, 221–228.
- Cusick, R.D., Kiely, P.D., Logan, B.E., 2010. A monetary comparison of energy recovered from microbial fuel cells and microbial electrolysis cells fed winery or domestic wastewaters. *Int. J. Hydrogen Energy* 35, 8855–8861.
- Deng, J., Jiang, J., Zhang, Y., Lin, X., Du, C., Xiong, Y., 2009.  $FeVO_4$  as a highly active heterogeneous Fenton-like catalyst towards the degradation of Orange II. *Appl. Catal. B* 84, 468–473.
- Figuerola, S., Vazquez, L., Alvarez-Gallegos, A., 2009. Decolorizing textile wastewater with Fenton's reagent electrogenerated with a solar photovoltaic cell. *Water Res.* 43, 283–294.
- Frigerio, N.A., 1963. An iodometric method for the macro- and microdetermination of peroxydisulfate. *Anal. Chem.* 35, 412–413.
- Fu, L., You, S.J., Zhang, G.Q., Yang, F.L., Fang, X.H., 2010. Degradation of azo dyes using in-situ Fenton reaction incorporated into  $H_2O_2$ -producing microbial fuel cell. *Chem. Eng. J.* 160, 164–169.
- Gupta, V.K., Suhas, 2009. Application of low-cost adsorbents for dye removal: a review. *J. Environ. Manage.* 90, 2313–2342.
- Hou, B., Sun, J., Hu, Y., 2011. Simultaneous Congo red decolorization and electricity generation in air-cathode single-chamber microbial fuel cell with different microfiltration, ultrafiltration and proton exchange membranes. *Bioresour. Technol.* 102, 4433–4438.
- Kolthoff, I.M., Medalia, A.L., Raaen, H.P., 1951. The reaction between ferrous iron and peroxides. IV. Reaction with potassium persulfate. *J. Am. Chem. Soc.* 73, 1733–1739.
- Li, L., Abe, Y., Kanagawa, K., Shoji, T., Mashino, T., Mochizuki, M., Tanaka, M., Miyata, N., 2007. Iron-chelating agents never suppress Fenton reaction but participate in quenching spin-trapped radicals. *Anal. Chim. Acta* 599, 315–319.
- Liang, C., Liang, C.P., Chen, C.C., 2009. pH dependence of persulfate activation by EDTA/Fe(III) for degradation of trichloroethylene. *J. Contam. Hydrol.* 106, 173–182.
- Liang, C.J., Bruell, C.J., Marley, M.C., Sperry, K.L., 2004a. Persulfate oxidation for in situ remediation of TCE. I. Activated by ferrous ion with and without a persulfate-thiosulfate redox couple. *Chemosphere* 55, 1213–1223.
- Liang, C.J., Bruell, C.J., Marley, M.C., Sperry, K.L., 2004b. Persulfate oxidation for in situ remediation of TCE. II. Activated by chelated ferrous ion. *Chemosphere* 55, 1225–1233.
- Liu, L., Li, F.B., Feng, C.H., Li, X.Z., 2009. Microbial fuel cell with an azo-dye-feeding cathode. *Appl. Microbiol. Biotechnol.* 85, 175–183.
- Lovely, D.R., Phillips, E.J.P., 1988. Novel mode of microbial energy metabolism: organism carbon oxidation coupled to dissimilatory reduction of iron and manganese. *Appl. Environ. Microbiol.* 54, 1472–1480.
- Nadim, F., Huang, K.C., Dahmani, A.M., 2006. Remediation of soil and ground water contaminated with PAH using heat and Fe(II)-EDTA catalyzed persulfate oxidation. *Water Air Soil Poll. Focus* 6, 227–232.
- Pirkanniemi, K., Metsärinne, S., Sillanpää, M., 2007. Degradation of EDTA and novel complexing agents in pulp and paper mill process and waste waters by Fenton's reagent. *J. Hazard. Mater.* 147, 556–561.
- Rittmann, B.E., 2008. Opportunities for renewable bioenergy using microorganisms. *Biotechnol. Bioeng.* 100, 203–212.
- Sun, J., Wang, X., Sun, J., Sun, R., Sun, S., Qiao, L., 2006. Photocatalytic degradation and kinetics of Orange G using nano-sized  $Sn(IV)/TiO_2/AC$  photocatalyst. *J. Mol. Catal. A* 260, 241–246.
- Sun, P.S., Li, C.J., Sun, J.H., 2009. Decolorization of an azo dye Orange G in aqueous solution by Fenton oxidation process: effect of system parameters and kinetic study. *J. Hazard. Mater.* 161, 1052–1057.
- Wang, Y., Niu, C.G., Zeng, G.M., Hu, W.J., Huang, Da Wei, Ruan, M., 2011. Microbial fuel cell using ferrous ion activated persulfate as a cathodic reactant. *Int. J. Hydrogen Energy* 36, 15344–15351.
- Wu, J., Wang, T., 2001. Ozonation of aqueous azo dye in a semi-batch reactor. *Water Res.* 35, 1093–1099.
- Xu, X.R., Li, X.Z., 2010. Degradation of azo dye Orange G in aqueous solutions by persulfate with ferrous ion. *Sep. Purif. Technol.* 72, 105–111.
- Yu, Z.Y., Keppner, H., Laub, D., Mielczarski, E., Mielczarski, J., Kiwi-Minsker, L., Renken, A., Kiwi, J., 2008. Photocatalytic discoloration of Methyl Orange on innovative parylene- $TiO_2$  flexible thin films under simulated sunlight. *Appl. Catal. B: Environ.* 79, 63–71.
- Yuan, R., Ramjaun, S.N., Wang, Z., Liu, J., 2011. Effects of chloride ion on degradation of Acid Orange 7 by sulfate radical-based advanced oxidation process: Implications for formation of chlorinated aromatic compounds. *J. Hazard. Mater.* 196, 173–179.